Structures 46 (2022) 214–232

Contents lists available at ScienceDirect

Structures

journal homepage: www.elsevier.com/locate/structures

Structural analysis of unreinforced masonry spiral staircases using Discrete Element modelling

A. Dell'Endice [a], M.J. DeJong [b], T. Van Mele [a], P. Block [a]

[a] ETH Zurich, Institute of Technology in Architecture, Zurich, Switzerland
[b] UC Berkeley, Department of Civil and Environmental Engineering, Berkeley, CA, USA

ARTICLE INFO

Keywords:
Cantilever spiral staircase
Unreinforced masonry
Discrete element modelling
Geometrical imperfections
Rigid blocks

ABSTRACT

Unreinforced masonry spiral staircases have been built for more than two thousand years in castles, churches and palaces, and these staircases require structural assessment. For a few decades, the structural behaviour of "cantilever" staircases has been debated among scholars. Several structural methods have been used, but due to the complex 3D geometry and the substantial number of treads, *a priori* assumptions have been made about the magnitude and point of application of the contact forces between the treads and the wall-tread connections. These assumptions influence the calculation of torsional moment, which, in some methods, reaches high values that could generate shear stresses greater than the material's strength. In this paper, a 3D model based on one helix of the "cantilever" spiral staircase of San Domingo de Bonaval, in Spain, has been analysed using the Discrete Element Method. The entire stair is analysed without making assumptions on the magnitude and location of the resultant contact forces, which are calculated for each tread using customised Python-based functions. The wall-tread connections have been modelled using rigid blocks, and several contact conditions have been investigated. Moreover, different friction angles and the influence of geometrical imperfections are analysed to simulate material tolerances and assembly imprecisions. The simulation results indicate that perfect wall-tread contact conditions lead to conservative predictions of the torsional moment. Instead, gaps and imperfections allow small displacements, which reduce the torque and increase compression forces in the inner helical ring of the stair. Low friction angles could increase the torsional moment values, while vertical settlements do not cause a significant effect. Cantilever situations could still occur due to not perfect contact conditions between consecutive treads, which suggests that the tread-tread contact area should be carefully inspected during restoration. More generally, this paper demonstrates the potential variability of the structural behaviour of highly indeterminate structures when boundary conditions are uncertain, while providing valuable context to inform restoration strategies.

1. Introduction

Unreinforced spiral staircases have been constructed for thousands of years. In the old testament, there is a short description of a spiral staircase inside the Temple of Solomon, which dates around 1000BCE Another well-known example is the staircase inside the Trajan's Column in Rome, built around 113 CE Throughout history, spiral staircases have been used mainly inside castles, helping to defend against attacks, and churches, where they were built inside walls and were part of a network of passages that allowed the carpenters to transport construction materials at the upper levels, eliminating the need of timber's scaffolding or other temporary structures [1]. The presence of spiral staircases in important buildings and their beauty promoted their use in the design of wealthy family homes until the end of the XIX century.

1.1. Structural features

The wide use of unreinforced spiral staircases contributed to the development of their geometrical and structural features. In the oldest examples, each tread was supported on the outside by the wall and on the inside by a central column. Later, more space was left between the flights. As a result, each tread was not connected to the same central column but supported by the tread below. Due to removing the central column, spiral staircases seemed to cantilever from the outer walls and were erroneously named "cantilever stairs". Andrea Palladio was in his book "Quattro Libri dell'Architettura" to mention the name "cantilever stairs" for the first time, describing the stairs he built in 1560 at the Accademia in Venice [2]. However, as already noticed by Goethe in his work *Italian Journey*: *"the stone steps are built into the wall and so tiered that each supports the one above it"* [3]. In most existing spiral staircases, it has been noticed that the tread embedment within the wall is usually

https://doi.org/10.1016/j.istruc.2022.10.070
Received 26 August 2022; Received in revised form 15 October 2022; Accepted 17 October 2022
2352-0124/© 2022 The Author(s). Published by Elsevier Ltd on behalf of Institution of Structural Engineers. This is an open access article under the CC BY-NC-ND license (http://creativecommons.org/licenses/by-nc-nd/4.0/).

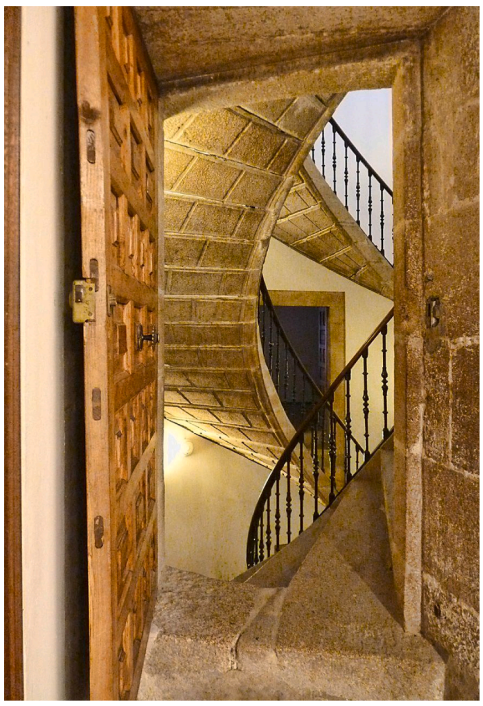

Fig. 1. Picture of a tread in correspondence of a door opening in the spiral staircase of the convent of San Domingo de Bonaval, Santiago de Compostela, Spain, XVII century.

about 10–15 cm, and only in a few cases, it reaches a length of 30 cm. This embedment length is often relatively short compared to the length of the treads, which can reach two meters. In addition, sometimes, the wall-tread area has windows or doors above, so there is no possibility to develop bending capacity in the socket (Fig. 1).

Considering these aspects, the primary internal force that must be resisted by each tread is the torsional moment, which occurs due to the eccentricity of the force transmitted by each tread to the one below and which needs to be resisted by the wall-tread connection. This behaviour is also combined with a compression effect in the inner ring of the stair as described by Angelillo and de Serio in [4,5]. Unlike many unreinforced masonry structures where the stone elements are mainly subject to compression, and where the stress is one or more orders of magnitude lower than the strength of the material, in spiral staircases, the shear stress caused by the torque must be evaluated in comparison to the tensile capacity of the material, which is limited. The internal torsion that must be resisted by each tread depends on a few aspects: i) how much force is transmitted by each tread to the tread below and; ii) the point of application of the resultant forces acting on each tread with respect to the barycentric axis. The torque causes internal shear stresses which depend on the cross-section geometry. Stones have a brittle behaviour when subject to tensile stress; [6] investigated the mechanical properties of stones and the presence of defects that can cause cracks. [7–10] described the structural behaviour of "cantilevered" staircases and the failure of treads in a flight where the treads at the base failed in torsion and consequently the treads above failed in bending, being no longer supported by the treads below. The inspection of the breaking surfaces also highlighted this type of failure due to tensile stress. Although the failures cases are relatively few, structural engineers still need to assess the existing spiral staircases, considering fire safety requirements. Indeed, in many historical buildings, spiral staircases represent the only vertical connection.

1.2. Related research

For a few decades, several scholars have investigated the structural behaviour of spiral stairs, primarily for assessment purposes. Several analysis methods have been applied: Heyman [11] analysed "cantilever" staircases, straight and spiral, considering that each tread transfers a certain amount of its weight to the tread below and assuming that the contact forces are located at the vertices of the solid representing the shape of the tread, and assuming a perfect wall-tread connection. According to Heyman's assumptions, the torsional moment increases linearly from the top to the bottom of the staircase, and can reach high values for long flights of stairs. [5] investigates the structural behaviour of the "cantilever" staircases of San Domingo de Bonaval in Spain, built in the XVII century, analysing one of the three helicoidal ramps. The same stair has been analysed in this paper. [5] solves for equilibrium through an optimization problem, minimising the potential energy, using constraints, equalities and inequalities, that represent small displacements and tolerances in the tread-wall connections or between the treads. Displacements and contact forces are determined at fixed points at the corners of the solid shape of the tread. The assumptions in De Serio et al. [5] result in a reduction of the torsional moment compared to Heyman's approach. More specifically, the torsion does not increase linearly down the whole set of stairs, but only increases for approximately the first 20 treads and remains relatively constant below that (Fig. 2). This behaviour is combined with a ring-like model, which produces the increase of compression forces in the inner ring of the stairs which locally corresponds to an increase of the axial forces along the length of each tread. Thus, the force regime inside the structure is compressive and determines the stress levels inside the elements well below the limit compressive and tensile strengths.

Meanwhile, [12] analysed straight and spiral "cantilever" staircases with rectangular cross-sections using the Discrete Element Method. Blocks were modelled as deformable and the wall-tread connections were simulated through specific displacement boundary conditions assumptions. However, the investigation is limited by computational constraints due to the use of deformable blocks, and the assumptions on the wall-tread connection do not allow the simulations of imperfect contact conditions.

So far, the analyses conducted on "cantilever" spiral staircases consist of two distinct phases: in the first phase, several assumptions are made on the magnitude of the forces transmitted by each tread to the one below and on the point of application of the resultant contact forces between the treads. As mentioned in the paragraph above, these two aspects influence the value of the torsional moment acting on the treads. In the second phase, the internal forces calculated in the first part are used to evaluate the stress state of the treads, considering the geometrical cross-section and the mechanical material properties. Although the second phase is relatively straightforward, the first part of the analysis remains affected by the solution method, the assumptions made on the point of application of the resultant contact forces, and by the wall-tread connection modelling. These assumptions are particularly important due to the high level of indeterminacy typical of unreinforced masonry structures, and to the geometrical complexity of spiral staircases. In this scenario, any small displacement or variation of the wall-tread or tread-tread contact conditions change the state of the internal forces due to the different position of the resultant contact forces. In this paper, a method to analyse "cantilever" staircases modelling the 3D geometry of the treads and the wall-tread connections with rigid blocks is proposed, without making a priori assumptions on the position of the resultant contact forces between the treads, which have been instead calculated for several wall-tread contact conditions, including the presence of geometrical deviations, and potential vertical settlements of the staircase.

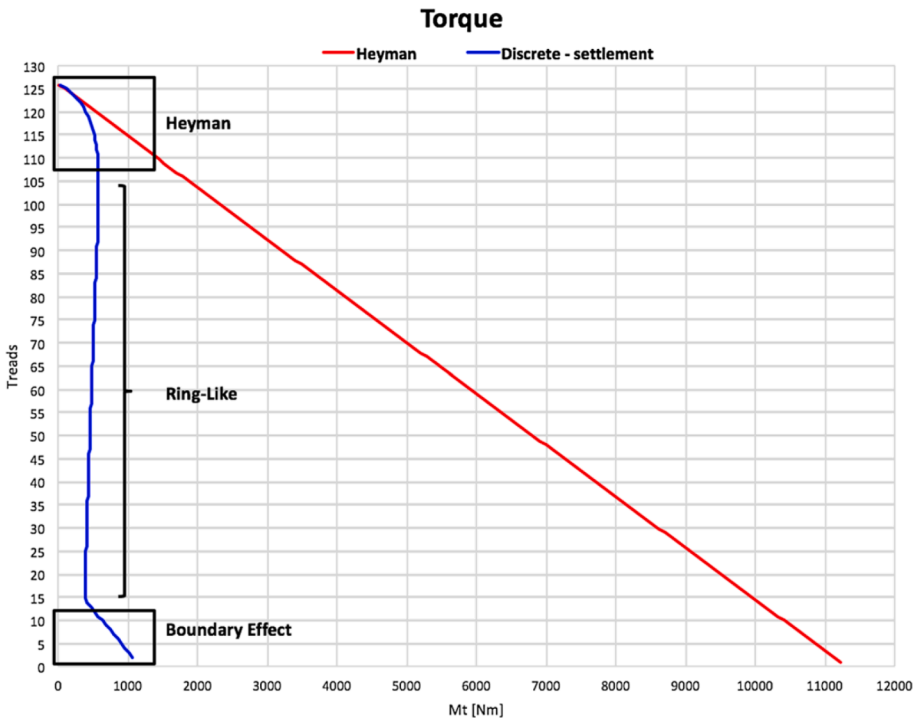

Fig. 2. Image taken from De Serio et al. [5]. Torsional moment values in the 126 treads of the spiral staircases of San Domingo de Bonaval calculated by De Serio et al. [5]. In blue, the values obtained through minimization of the potential energy, allowing settlements of the treads; in red, the torque values calculated by De Serio et al. [5] considering Heyman's approach in Heyman [11].

2. Methodology

In this paper, one helix based on the spiral staircase built by Domingo de Andrade in the XVII century, inside the convent of San Domingo de Bonaval, located in Santiago de Compostela, in Spain, has been analysed. First, the treads and the external supporting wall have been modelled with 3D solid meshes using the open-source, Python-based computational framework *compas* [13]. The structure has been then analysed with the Discrete Element Modelling method, using the commercial software 3DEC by Itasca [14–16]. Then, 3DEC's results have been post-processed using customised python-based functions, developed in *compas* and COMPAS Masonry [17], to compute the position and magnitude of the resultant contact forces and the internal forces in each tread.

2.1. 3D modelling

The 3D model of the staircase analysed is based on the model used by De Serio et al. [5]. However, since in De Serio et al. [5] a simplified version of the actual geometry has been used, which is not suitable for a DEM analysis in 3DEC, in the current paper, the treads have been modelled considering the accurate description of the same staircase made by Cabo et al. [18]. According to [18], each tread is supported at one end by the wall and, at the other end by the tread below, through a protrusion that overlaps with the previous tread.

Fig. 3 shows that for some treads there is no overlapping over the tread length between the protrusion and the wall socket. This particular geometrical feature, not very common in spiral staircases, is also discussed by Cabo et al. [18], which hypothesizes two scenarios: a) in the first one, the designer, Domingo de Andrade, could have left on purpose

Fig. 3. Gaps between the treads in the spiral staircase of San Domingo de Bonaval, Santiago de Compostela, Spain, XVII c.

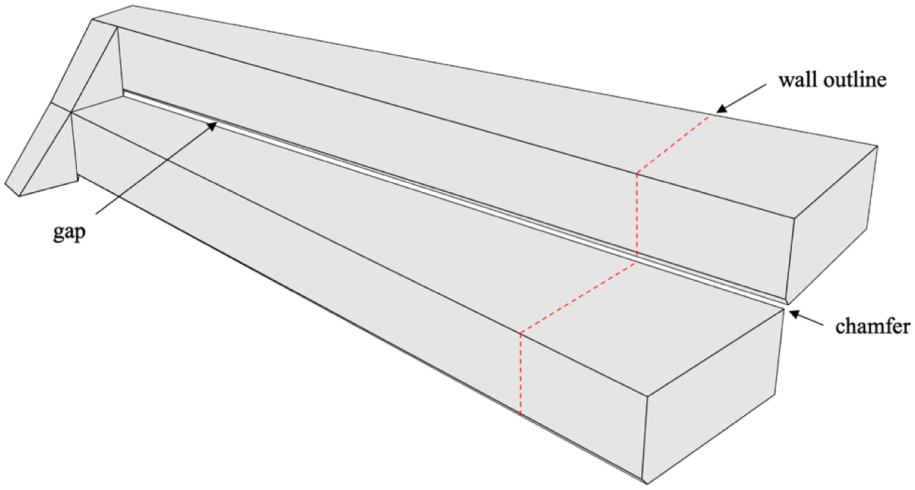

Fig. 4. Digital model of the treads showing the gap created by chamfering the bottom front edge.

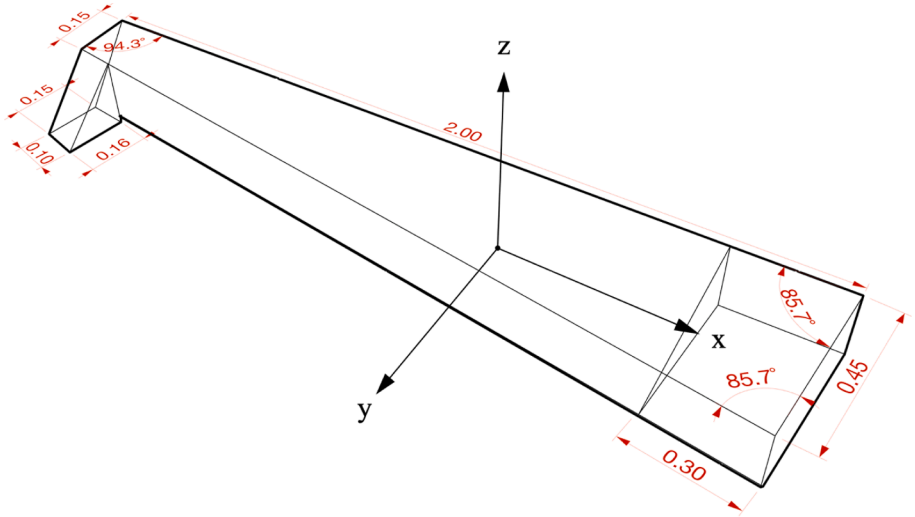

Fig. 5. Dimensions of the treads and local reference system.

a gap to let the light go through the treads; b) in the second one, the author supposes that the tiny overlapping areas between the treads were filled by mortar, which decayed with time. For this reason, in the current work, to better simulate the effect due to the unusual geometry of the treads, a chamfer has been introduced in the central area of each tread (Fig. 4) to avoid any edge-to-edge contact between them. Later, to understand the influence of continuous contacts along the treads, another model was generated overlapping the treads by 2 cm and analysed, as described in Sections 3.6–3.7. The entire model consists of 6469 3D solid meshes: there are 126 treads, which dimensions are illustrated in Fig. 5, and all the other blocks make up the supporting exterior wall and the support ring at the base of the tower (Fig. 6). The

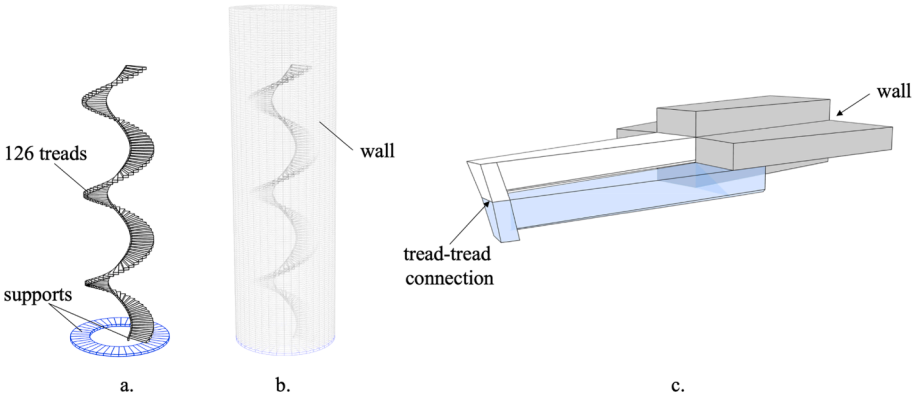

Fig. 6. (a) Treads and supports. (b) Wall blocks around the stair. (c) Tread in contact with the tread below and the surrounding wall.

blocks composing the exterior wall are not constrained as fixed in the simulation. Therefore, during the calculation, they can slightly move vertically under their self-weight due to the joints' elasticity. However, their global vertical displacements are almost negligible due to the high values of joint stiffness applied (as explained in Section 2.2) and their perfect digital geometry.

2.2. Discrete Element modelling

The structural analysis has been conducted using the Discrete Element Modelling (DEM) method through the commercial software 3DEC by Itasca. The DEM method has been introduced for a few decades for the structural analysis of several engineering problems dealing with discrete structures (soil mechanics, particles, masonry, etc.) and has several applications in the field of masonry structures [19–22]. The DEM algorithm in 3DEC is based on the integration of the equation of motion in the time domain using the central difference method, which is an explicit method. Therefore, a large amount of damping has to be introduced in the equation of motion to deal with static or quasi-static analyses [23]. In this paper, to reach the equilibrium faster, viscous damping has been used in 3DEC, which through an adaptive scheme, considers mass-proportional damping to ensure a faster convergence to the solution. The peculiarities of this method - i) the discretised elements can move and deform independently; ii) large displacements are possible; iii) the blocks can detach from each other or form new contacts - make it suitable for the structural assessment and design [24–26] of unreinforced masonry structures. Indeed, in DEM, Heyman's fundamental assumptions on the "material" masonry [27] can be approximated [23,28,29], namely: no tensile strength, unlimited compressive strength and no sliding. The no tensile condition is considered by eliminating the tensile strength and cohesion in the Mohr-Coulomb criterion applied to the joints; the use of rigid blocks implies unlimited compressive strength for the blocks, and the no sliding condition is satisfied by using high friction angles or enforced by the 3D stereotomy. Although, as mentioned in section 1.2, in spiral staircases, the evaluation of the internal stress state is crucial to calculate the ratio between the tensile strength of the material and the stress applied, the analysis has been conducted on rigid blocks. Rigid blocks have the advantage of being less computational demanding in the case of complex 3D geometries with many elements. The analysis with rigid blocks gives, as initial output, the global equilibrium of the structure without considering the potential breaking of the material, but it also returns the contact forces acting in between the treads for each vertex of the 3D solid meshes. The contact forces have been post-processed using customised Python-based *compas* functions, calculating the point of application, magnitude and direction of the resultant forces in the wall-tread connections and in between the treads. In this way, it is possible to follow the contact forces during the simulation of several boundary conditions, together with different friction angles, following the variations in the structural behaviour of the spiral staircase. Furthermore, this strategy allows using a more realistic model where each tread is surrounded by blocks and avoids approximating the wall-tread connection through displacement or stiffness boundary conditions assumptions. The resultant contact forces have been then used to calculate the internal forces, namely axial and shear forces and torsional and bending moments. The parametric model used allowed the evaluation of the internal forces at any location along the length. Specifically, for this work, the entire length has been subdivided by 100, and thus, the internal forces are evaluated every 2 cm. Afterwards, only the treads with the highest internal forces were checked by calculating the internal stress state locally, based on the specific cross-section. In the analysis setup, the material properties applied to the rigid blocks are the same as [5], with a density of 2700 Kg/m^3 and a Young Modulus of 24 GPa. Three different friction angles have been used, 20°, 30° and 40°, to evaluate the effect on the internal forces. The joint stiffness values, normal and shear, have been calculated according to [22,30], considering a joint space equal to the height of the blocks (19 cm).

$$J_{kn} = \frac{E}{h_{block}}, \tag{1}$$

where J_{kn} is the normal joint stiffness, E is the Young's modulus of the material, h_{block} is the block height. For the evaluation of the joint shear stiffness, the E (Young's modulus) has been replaced by G (shear modulus), which has been evaluated according to (2):

$$G_{block} = \frac{E}{2(1+\upsilon)}, \tag{2}$$

where υ is the Poisson's ratio considered equal to 0.2.

Then, the value of the shear joint stiffness has been evaluated as in [22]:

$$J_{ks} = \frac{G}{h_{block}} \tag{3}$$

The shear strength at the joints is governed by friction according to the Mohr-Coulomb failure criterion:

$$\tau = \sigma \, tan(\phi), \tag{4}$$

where τ is the shear strength, σ is the normal stress, ϕ is the friction angle. The cohesion has been neglected.

In previous studies [22,31,32], joint stiffness values have sometimes been decreased to reduce the computational time. In this work, the calculated joint stiffness values from (1) and (3) have been used without decreasing them. In this way, the joint stiffness is kept out of the parametric analysis, and the high values used have reduced the effect of the elasticity lumped at the joints. Indeed, the total vertical displacement at the top of the entire tower (treads plus exterior wall), subject to self-weight, is about 0.5 mm due to the joint stiffness effect. So, the uncertainty in the wall-tread conditions have not been modelled by varying the stiffness of the joints, but this has been considered geometrically, as shown in the following paragraphs. Gravity has been gradually applied in ten steps at the beginning of each analysis to avoid dynamic effects.

2.3. Boundary conditions

In highly indeterminate structures such as spiral staircases, the implemented methodology allows to simulate and evaluate the effect of the variation of the boundary conditions. The goal is not to define the structure's actual stress state, which is impossible to know, but to understand the trends and limits reached by the internal forces in some of the conditions the structure experience. The design of the boundary conditions has been done keeping in mind the construction process of "cantilever"" staircases, simulating plausible cases. Historically, from an assembly point of view, the construction was done completing one "layer" at the time [1], where each layer contains the tread and the wall blocks around it. The construction sequence of the stair under investigation has also been simulated by Cabo et al. [18] using a physical scale model of a few treads together with the outer wall. The experimental tests conducted by Cabo et al. [18] confirm the feasibility of a layer-by-layer assembly process without the need to shore the treads temporarily (Fig. 7).

In this construction process, it seems evident that the masons always tried to place each tread at least in contact with the one below and with the base of the wall socket. The design of the boundary conditions takes into account these considerations. As a result, it can be deduced that tolerances exist between the lateral and top surfaces of the tread and the wall socket (t1,t2 and t4 in Fig. 8a and Fig. 9), and cantilevering situations could only occur as a result of successive displacements or settlements, which locally modify the contact conditions at the bottom of each tread, especially in the tread-tread connection.

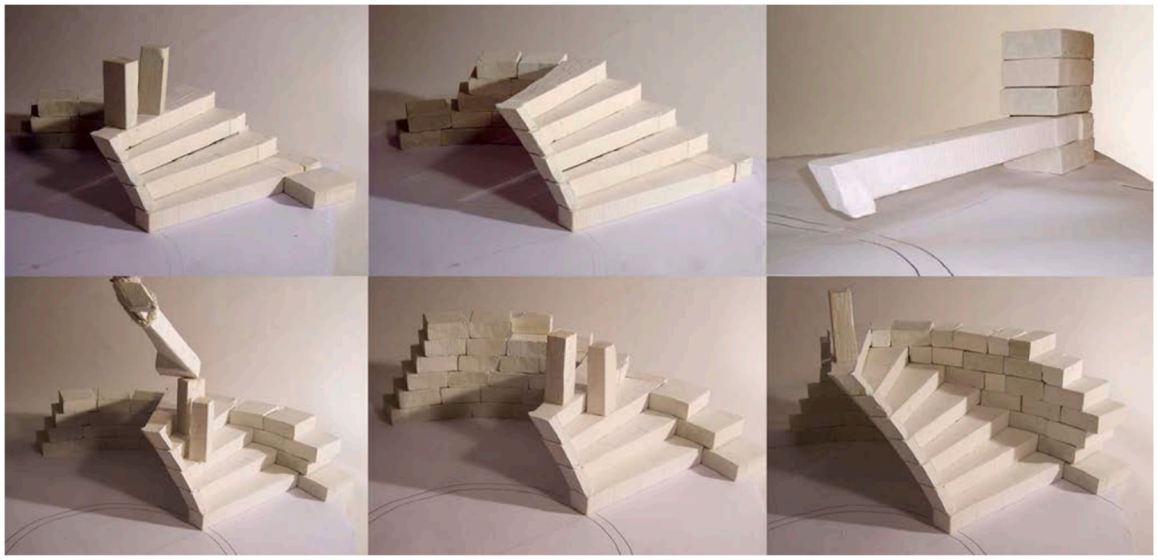

Fig. 7. Sequence of experimental tests conducted by Cabo et al. [18] on the spiral staircase under investigation in the current work to simulate the construction sequence.

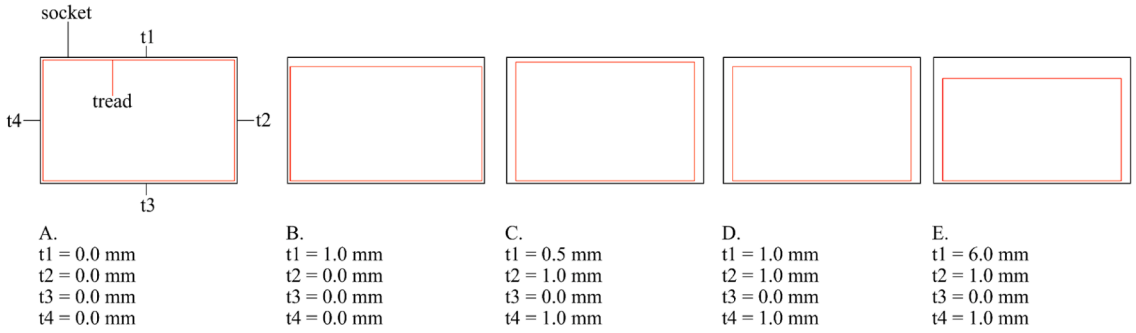

Fig. 8. (a) No clearance. All the tolerances t1,t2,t3, and t4 are equal to zero; the tread and the wall are in perfect contact. (b) Clearance at the top of the wall-tread connection; t1 equal to 1 mm and t2, t3 and t4 equal zero. (c) Clearance at the top and on the lateral joints of the wall-tread connection; t1 equal to 0.5 mm, t2 and t4 equal to 1 mm and t3 equal to zero. (d) Same as (c) but with t1 equal to 1 mm. (e) Same as (c) and (d) but with t1 equal to 6 mm.

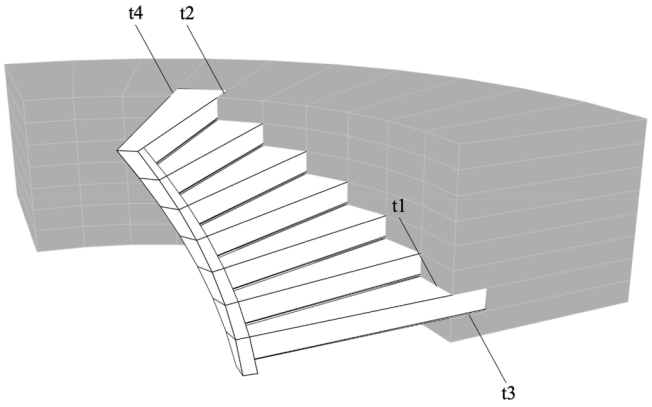

Fig. 9. Close-up of a portion of the spiral staircase with the location of t1,t2, t3,t4.

2.3.1. *Wall-tread connection*

The analysed wall-tread contact cases cover a range of real situations regarding the condition of the wall-tread connection. Five cases, A to E, have been considered, as shown in Fig. 8.

2.3.2. *Geometrical imperfections*

Geometrical imperfections exist in every structure. Defects, fabrication tolerances, and manual adjustments cause slight geometrical variations in the blocks, leading to not perfect contact conditions between them [32,33]. Since the contact conditions in the wall-tread connection and in between the treads are crucial for the behaviour of the staircase, an investigation has been conducted to understand their impact. Imperfections have been applied to the treads, only in the model with no clearance generating more realistic and unpredictable tolerances. For each tread, the geometrical imperfections have been applied to the vertices of the solid 3D mesh. The vertices have been first subdivided into two categories related to their position: the first group "A" contains the vertices belonging to the tread-tread connection; the second group "B" includes the vertices of the tread in contact with the wall socket (Fig. 10).

The application of the imperfections consists of moving each vertex in the negative direction (i.e. towards the inside of the tread) along the direction of the vertex normal. The vertex normal has been evaluated as the weighted average of the normals of the neighbouring faces. The displacement value for each vertex has been picked randomly, using a uniform distribution, in a specific range. A different range of imperfections has been assigned to each of the two groups ("A" and "B"); smaller imperfections for the first group (tread-tread connection) and larger imperfections for the second (wall-tread). The reason behind this choice is to avoid imperfections that could cause a condition where the tread is

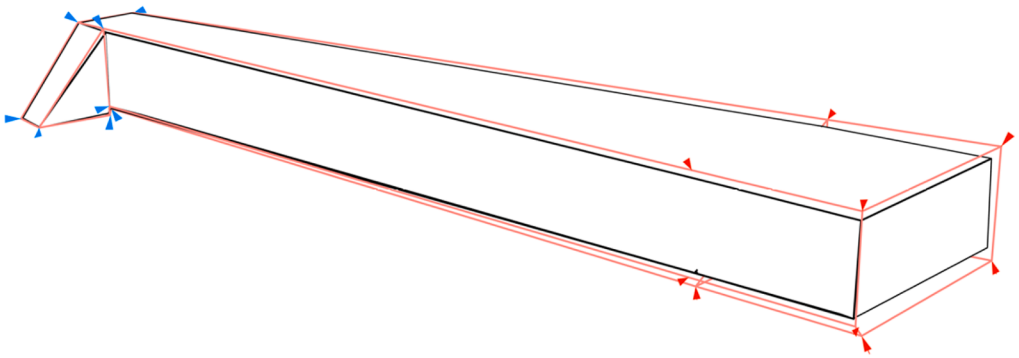

Fig. 10. Example of geometrical deviations on a single tread. The pink wireframe represents the original shape of the tread, while the black wireframe the shape after the application of imperfections. The blue arrows indicate the vertices of the tread-tread area (smaller deviations applied), whereas the red arrows represent the vertices of the wall-tread socket (subject to more significant deviations). Just for clarity, in this figure, the deviation used has been amplified compared to the values used in this paper.

Table 1
Values of the geometrical deviations applied.

Set 1				
Cases	Range group "A" [m]		Range group "B" [m]	
i1a - i1b - i1c	0.0	0.0005	0.00051	0.001
Set 2				
Cases	Range group "A" [m]		Range group "B" [m]	
i2a - i2b - i2c	0.001	0.0015	0.0016	0.002

cantilevering from the wall. As already mentioned in paragraph 2.3, the authors supposed that during construction, the treads, even with imperfections, were always placed touching the previous one and touching at least the base of the wall-tread connection. For this work, two sets of ranges have been considered for each of the two groups of vertices, as shown in Table 1. Each set has been replicated three times to generate different random cases from the same imperfections range.

2.3.3. *Vertical settlements*

The last variation of boundary conditions investigated in this work concerns the effect of vertical settlements, which could have occurred over a long period of time, or right after construction, due to the forces travelling down along the central spiral ring.

The vertical settlement of the central support (Fig. 11) has been applied to all the models with clearance and imperfections.

The displacement has been simulated in 3DEC in steps of 0.0005 mm each, in a negative Z direction. At the end of each step, the velocity has been set to zero, and the global equilibrium of the entire structure has been calculated. The number of steps, namely the total displacement applied to each model, depends on the size of the tolerance t1 (Fig. 12 top). The maximum possible vertical displacement values **δ** (listed in Table 2) have been evaluated considering the maximum allowed rotation until the top part of the tread touches the intrados of the wall-tread connection (Fig. 12 bottom). Indeed, this should be avoided because if the tread starts working as a cantilever, the vertical force travelling in the central ring, which is responsible for the settlement, would not be transferred to the central support.

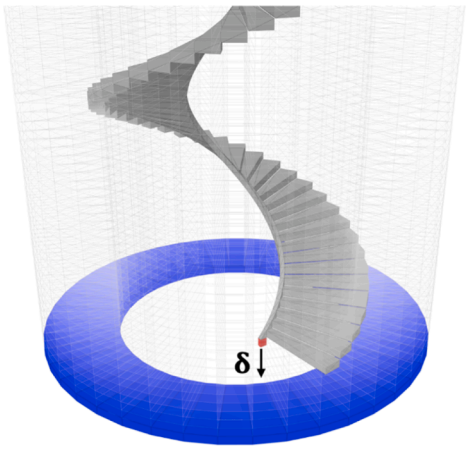

Fig. 11. Vertical displacement of the central support.

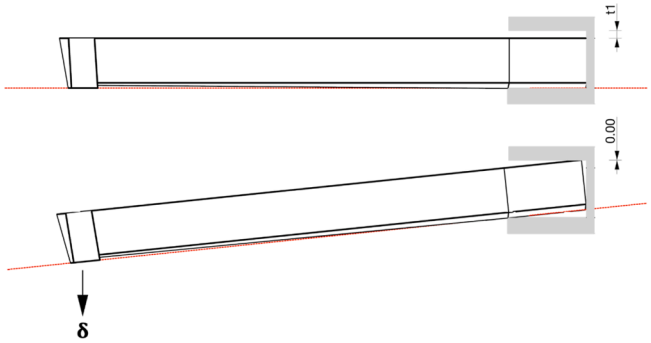

Fig. 12. (Top) the initial position of the tread in the configurations with tolerance t1 between the tread and the socket. (Bottom) max vertical displacement δ, which minimises the value of t1 (tread touching the socket). For clarity, in this figure, the displacement δ has been amplified compared to the actually applied displacement.

Table 2
Values of the maximum possible vertical displacements δ allowed by each configuration analysed.

Wall-tread connection	Max possible vertical displacement (δ) [m]
"B"	0.0056
"C"	0.0028
"D"	0.0056
"E"	0.034

3. Results and discussion

In this section, the results of the parametric analysis are presented. In addition, the implemented post-processing of the 3DEC results allows calculation and visualization, for each boundary condition, of the magnitude and point of application of the forces acting on each tread of the stair, which clarifies the related structural behaviour.

The resultant contact forces have been then used to calculate the internal forces along the entire length of each tread, with respect to the local barycentric axis and reference system (Fig. 5). Three friction angles, namely 20°- 30°- 40°, have been used in the analysis.

3.1. Contact forces

All the simulated wall-tread boundary conditions are characterised by a specific configuration of the contact forces, which highlights the sensitivity of the structure to contact conditions, imperfections and friction angle. Fig. 13 shows the resultant contact forces applied to tread n70, counting from the bottom of the stair, for the wall-tread condition cases A, B, C, E, Imperfection 1 and Imperfection 2, subject to self-weight.

For each case, the contact force configuration slightly varies along the stair due to small rotations and translations of the treads.

In condition "A" (Fig. 13-A) the no-clearance in the socket limits the displacement of the tread. Reactions **a** and **b** are in the centre of the contact area with the above and below treads producing a clockwise rotation, which is counterbalanced by the anti-clockwise rotation caused by the couple **c**-**d**. The reactions **c** and **d** have a significant magnitude because, since there is no clearance, part of the weight of the wall above acts on the tread. The reactions **e** and **f** correspond to the contact forces with the lateral sides of the wall-tread socket. Finally, the contact force **g** between the backside of the tread and the wall is due to a small vertical downward displacement of the tread at the inner ring.

In condition "B" (Fig. 13-B), where 1 mm clearance is introduced at the top of the tread, reaction **c** disappears, and the couple **e**-**f** counterbalances the clockwise rotation due to the couple **a**-**b**. Due to the larger clearance which cause a higher downward displacement of the tread, reaction d moves at the edge of the wall-tread connection, forming a couple with the self-weight **w** of the tread. Reaction **g** in the back, moves as well on the right side. It is worth noticing that the larger rotation allowed, moves reactions **a** and **b** towards the tread below (left side), and this phenomenon is even more evident in condition "C", where the tread has clearance at the top and on the sides, and it is freer to rotate.

Indeed, in this case, **a** and **b** are on the left edge of the tread-tread contact area. Since there is no lateral contact in the wall-tread socket, the clockwise rotation due to the couple **a**-**b** is taken by the anti-clockwise rotation due to **c**-**d**. In this case, since the top tolerance t1 is tiny (0.5 mm), the tread rotation generates the contact force **c** at the top left corner.

In configuration "E" (Fig. 13-E), the tolerances do not allow any contact with the lateral sides of the socket and with the top (t1 = 6 mm). In this case, the torque generated by the couple **a**-**b** is only counterbalanced by the couple **w**-**d**. Indeed, looking at the torsional moment along the whole stairs (Fig. 16a), the values reached, for almost all the treads, are bounded from below and correspond to the self-weight of the tread multiplied by the moment arm, which is half the tread's width from the barycentric axis to the point where force **d** acts.

Finally, for the two cases with imperfections (1 and 2), there is variability of the actual socket conditions, and the reaction forces are in locations that are difficult to predict a priori.

3.2. Internal forces and the effect of the friction angle

As mentioned above, the location of the resultant contact forces and their magnitude have an influence on the internal forces in each tread. Thus, the normal and shear forces and the bending and torsional moments have been calculated along the entire length of each tread. Fig. 14 shows the diagrams of the axial force and torsional moment for steps

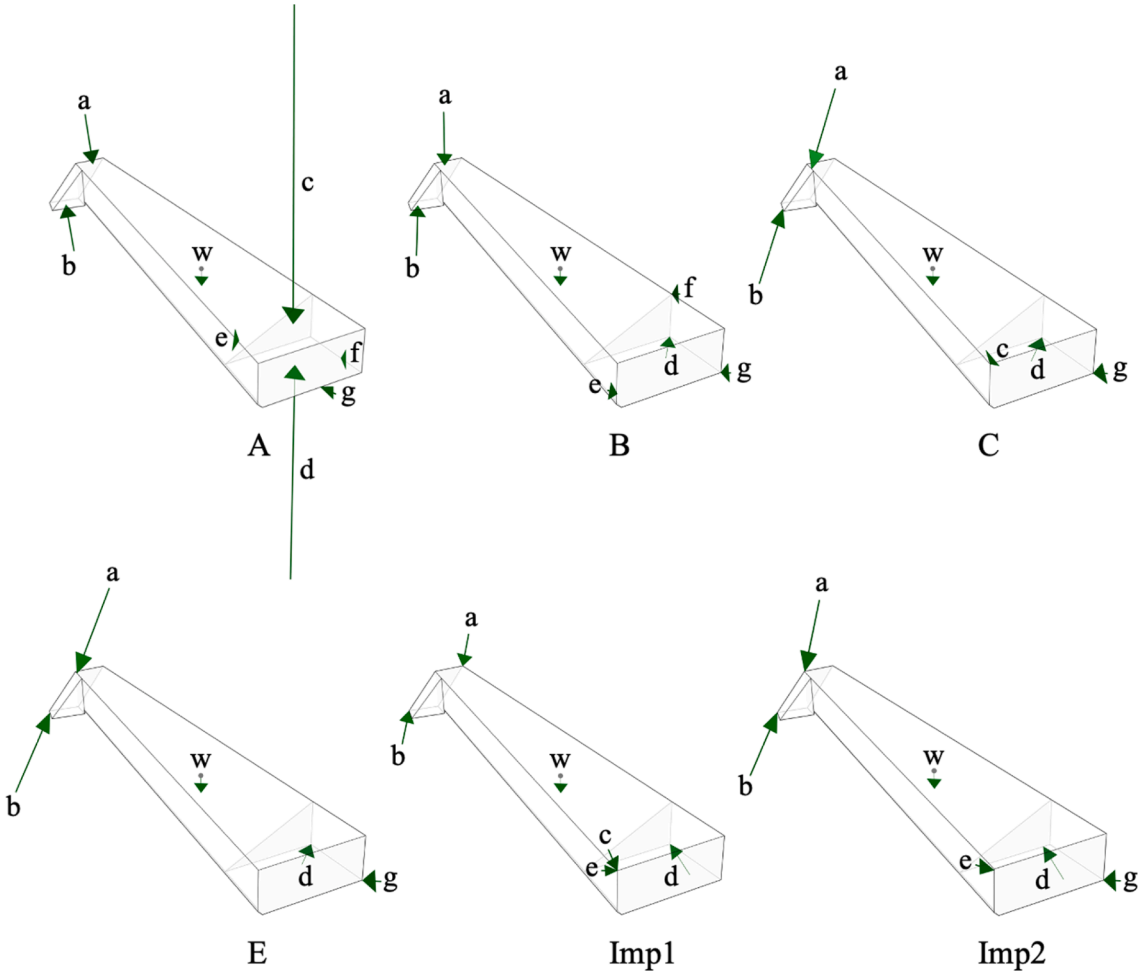

Fig. 13. Contact forces on the 70th tread for each of the six wall-tread contact conditions analysed.

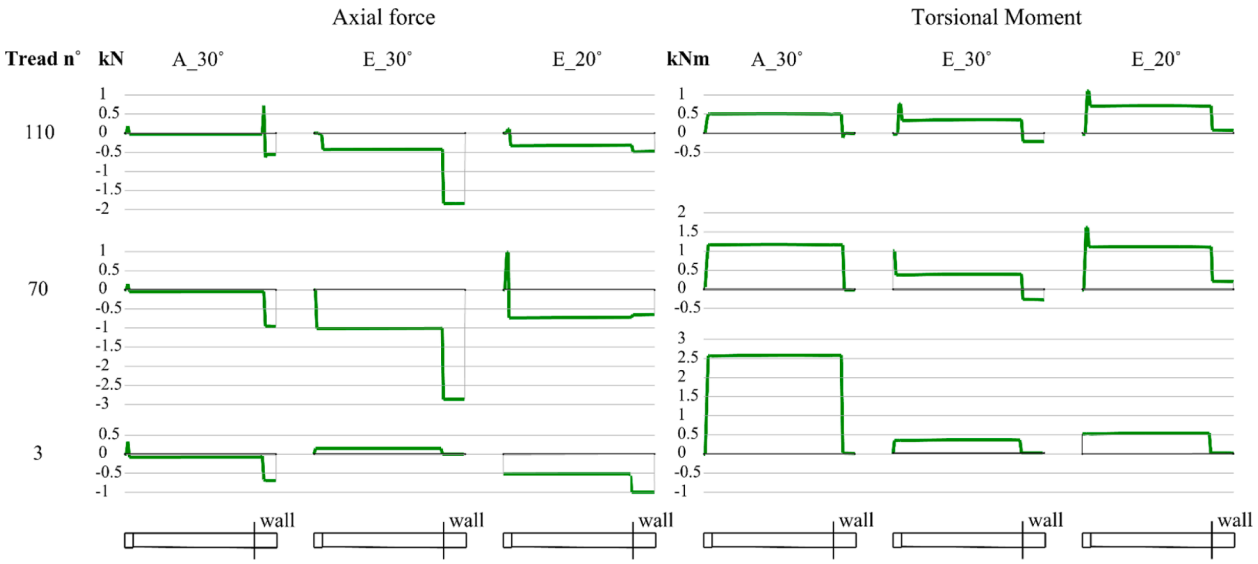

Fig. 14. Diagrams of the axial force and torsional moment for steps n°3-70-110, for wall-tread conditions: "A" with friction angle 30° and "E" with friction angles 30° and 20°.

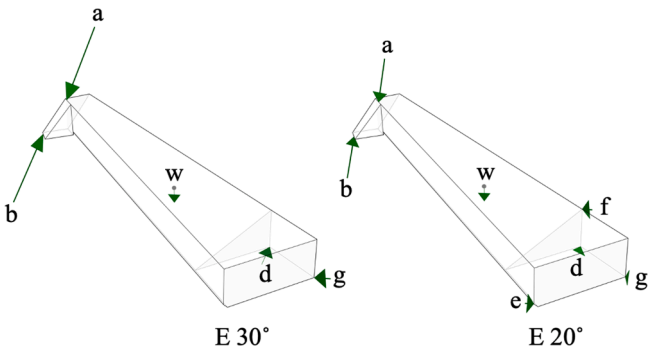

Fig. 15. Contact forces on the 70th tread from the bottom, for the wall-tread contact condition "E". a) Friction angle 30°. b) Friction angle 20°.

numbers 3, 70, and 110, for the two extreme wall-tread conditions: "A" with friction angle 30° and "E" with friction angles 30° and 20°.

Fig. 14 clarifies how a less tight socket ("E_30") decreases the amount of torque and increases the axial force in the treads, as also shown by De Serio et al. [5]. On the other hand, it is interesting to notice the effect of a friction angle of 20° on case "E". While for case "A", with no clearance in the socket, a lower or higher friction angle did not show any variation of the internal forces, for all the other cases decreasing the friction angle causes a slight reduction of the axial force and increases the torsional moment to values comparable, for steps 70 and 110, to the one reached by case "A_30". As shown in Fig. 15, with a lower friction angle, forces **a** and **b** change their directions, the tread engages the lateral sides of the socket (forces **e** and **f**) and the torque increases.

More in detail, Fig. 16a shows for the wall-tread contact conditions A-B-C-D-E, the torsional moment values at the middle section of each of the 126 treads, for the case with friction angle equal to 30°.

From the diagram in Fig. 16a, the amount of torque generated by the couple **a**-**b** (Fig. 13) and transmitted through the tread cross-section is inversely proportional to the level of tightness of the wall-tread socket. Indeed, the torque decreases going from condition "A" to condition "E". For case "E" (tread not touching the sides and the top of the socket), the magnitude of the torque is the smallest, and corresponds to the self-weight of the tread multiplied by the moment arm (half of the tread's width in correspondence of the wall socket). The tolerances used in case "E" are similar to the ones used by De Serio et al. [5], and the torsional moment values are almost identical.

Of all the cases analysed, the maximum torque occurs in the case with no clearance, where the torque increases from the top to the bottom of the stair. However, in this case, which is comparable to Heyman's assumptions [11] about perfect wall tread-contact conditions, the torque does not reach the values calculated by De Serio et al. [5] following Heyman's strategy.

Meanwhile, the diagram in Fig. 16b shows the effect of the friction angle on the torsional moment values for case E. As already mentioned at the beginning of this paragraph, a lower friction angle (case E_20°) increases the displacement of each tread (Fig. 17a-*b*-c), and, even in the cases with higher tolerances, the treads can rotate and engage the socket, increasing the torsional moment values.

Indeed, the introduction of tolerances in the wall-tread socket increases the magnitude of the contact forces travelling along the inner ring of the stairs and changes their directions (Fig. 18a-*b*-c). However, it is worth noticing that in both cases (with and without clearance), the ring force is relatively low compared to the total self-weight of the treads above, indicating that most of the weight is transferred to the wall. This mostly depends on the geometry of the treads, the position of the centre of mass and the features of the overlapping area between treads, and it needs to be evaluated case by case.

Depending on whether the treads have clearance to move, or alternatively a low friction angle, they could either engage the socket or not. Engaging the socket increases the torsional moment; otherwise, a minimum torsional moment is observed. Fig. 19 describes, for the case "E", the effect of friction angle on the ring and wall force components. For 30°, the treads do not move enough to engage the socket, and the resultant y components of the contact forces in the wall-tread area do not increase (Fig. 19c), meaning that the treads reach the minimum torque value and do not touch the top or the sides of the socket. As explained in paragraph 3.1, in this case, the couple **a**-**b** is only counterbalanced by the couple **w**-**d**. On the other hand, in the case of 20°, the displacement of the treads allows engaging the socket laterally. Indeed, the resultant y components of the contact forces in the wall-tread area increase (Fig. 19c), and the couple **e**-**f** also counterbalances **a**-**b**.

Finally, regarding the bending moment, since there are no cantilever situations in the models without geometrical imperfections, the treads always are in contact with each other. Therefore, the value of the bending moment, measured in the section at the beginning of the wall-tread socket, is almost constant along the whole stair and does not reach significant values, as described in paragraph 3.6.

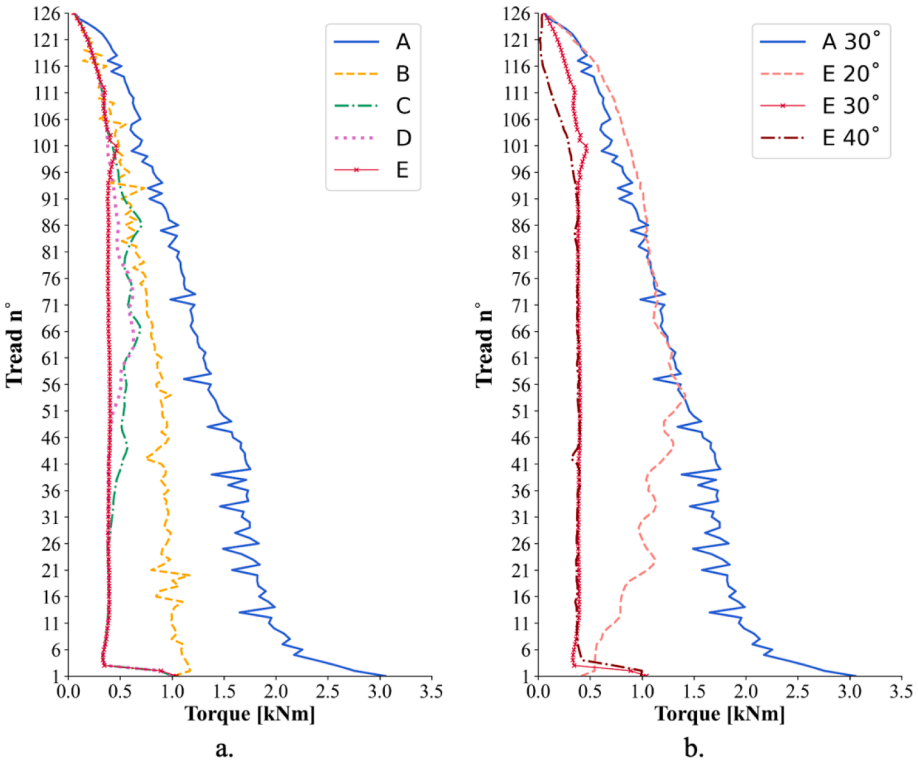

Fig. 16. Torsional moment values in the whole staircase for the wall-tread contact conditions with perfect geometry: a) "A-B-C-D-E" with friction angle equal to 30°; b) "A" with friction angle 30° compared to "E" with friction angles equal to 20°, 30° and 40°.

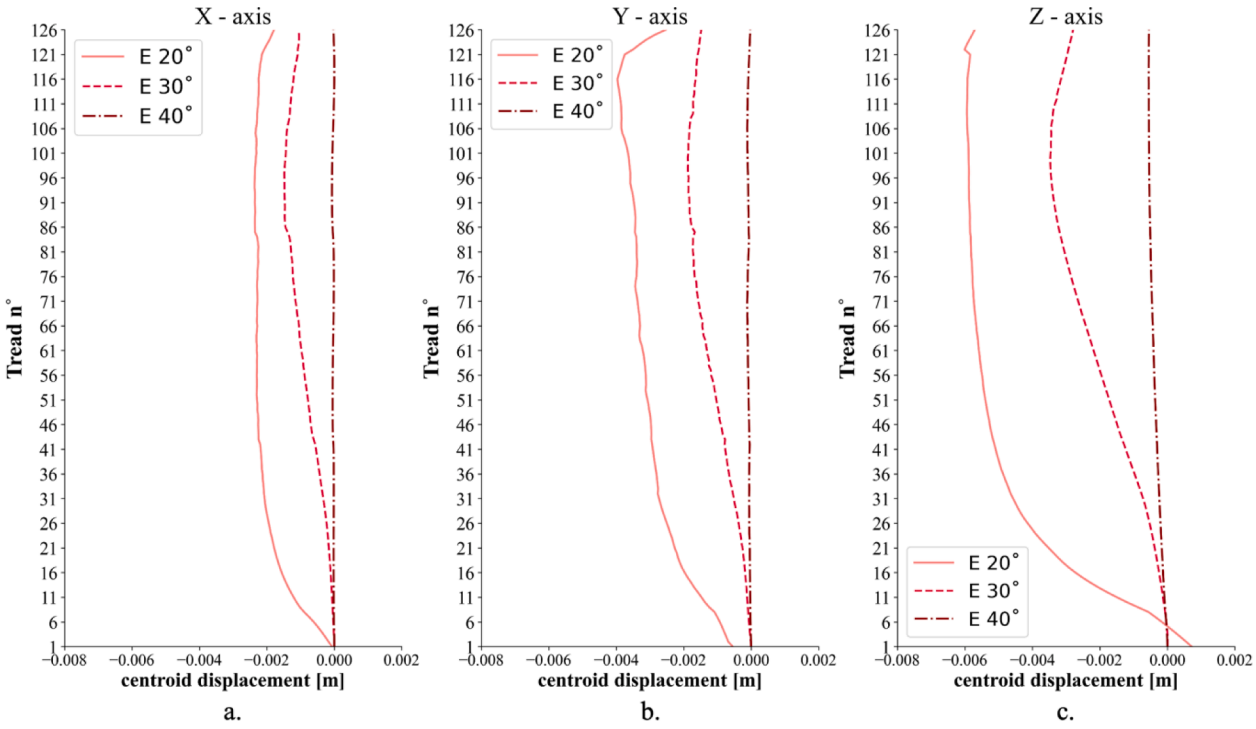

Fig. 17. Centroid translation components ×, y, z referred to the local reference system of each tread for the wall-tread contact conditions "E" and for friction angles 20°, 30° and 40°.

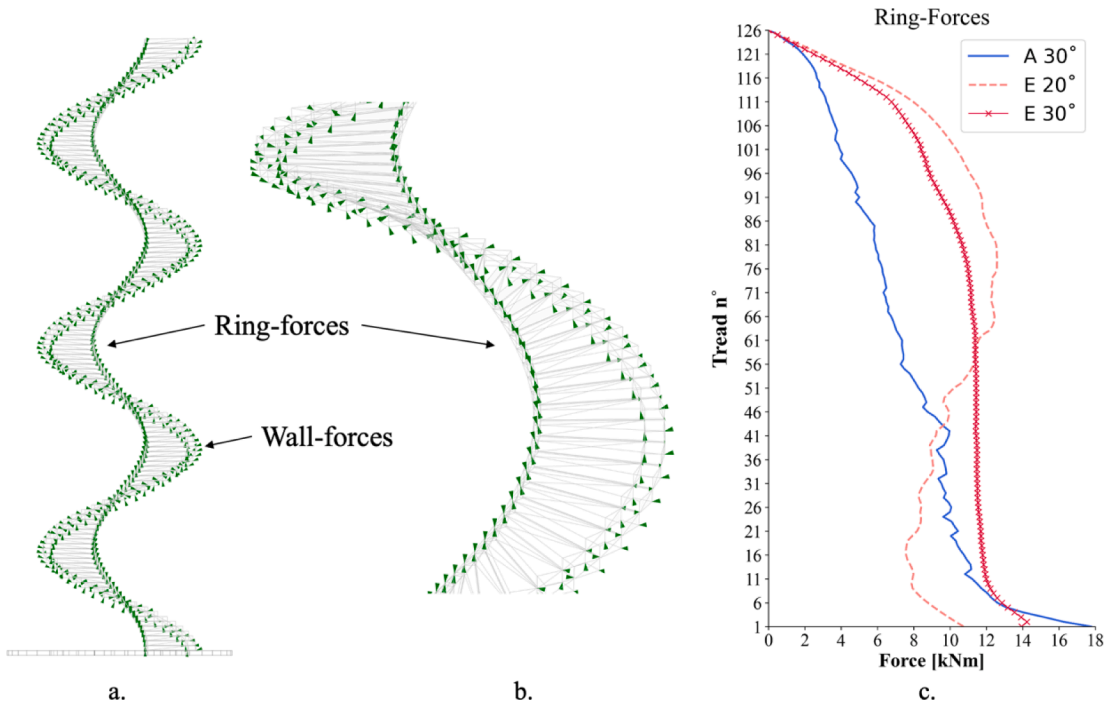

Fig. 18. a) and b) visualisation of the resultant contact forces within the treads. c) Magnitude of the resultant contact forces travelling along the central ring for case "A", "E_20" and "E_30".

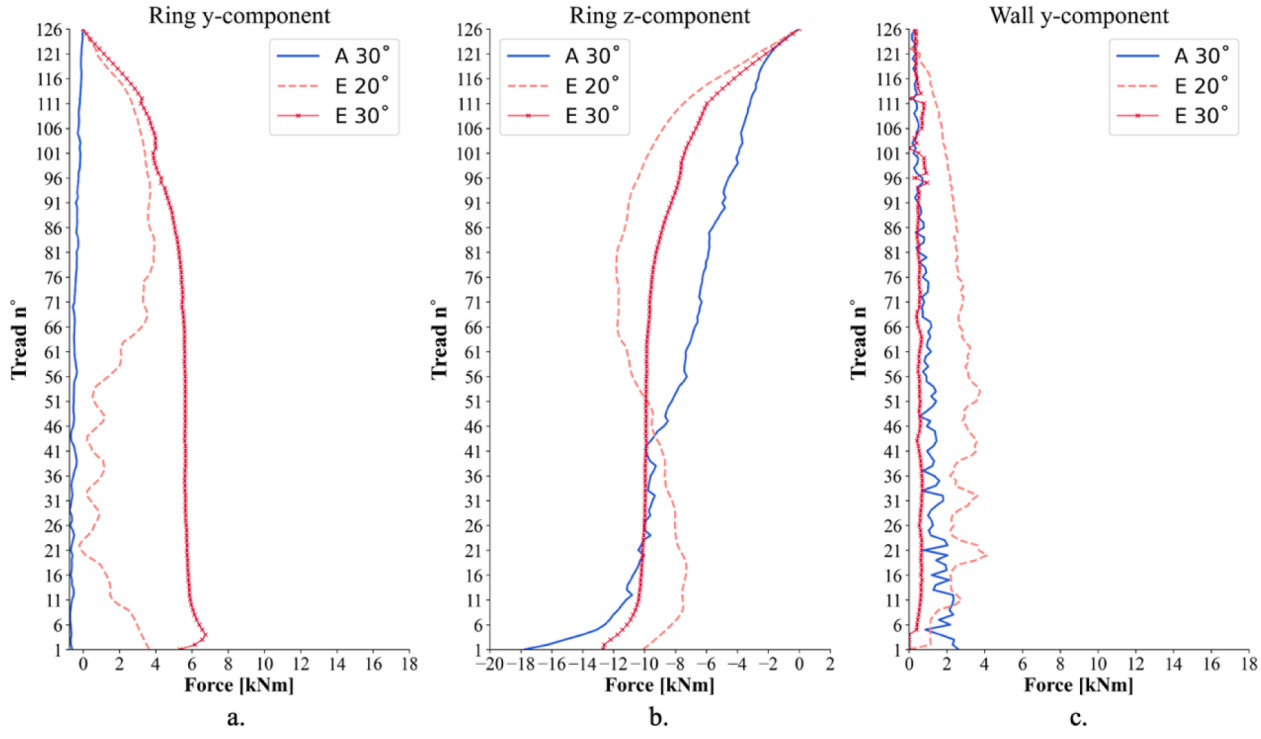

Fig. 19. a) Magnitude of the ring forces (y component acting at the top of each tread). b) Magnitude of the ring forces (z component acting at the top of each tread). c) Magnitude of the resultant wall forces (y component per tread).

3.3. Geometrical imperfections

The analysis results with geometrical imperfections highlight the potential importance of defects in the contact conditions. Indeed, the introduction of geometrical deviations not only causes different levels of tightness in the wall-tread socket but brings randomness to the contact conditions. Fig. 20a and 20b, respectively, show the torque values for the two sets of imperfections applied (set1 and set2), compared to the case "A" and "E", which represents the upper and lower bounds of the torsional moment values found previously.

Fig. 20a and b show that the magnitude of the geometrical imperfections, which influences the tightness of the socket, produces the same

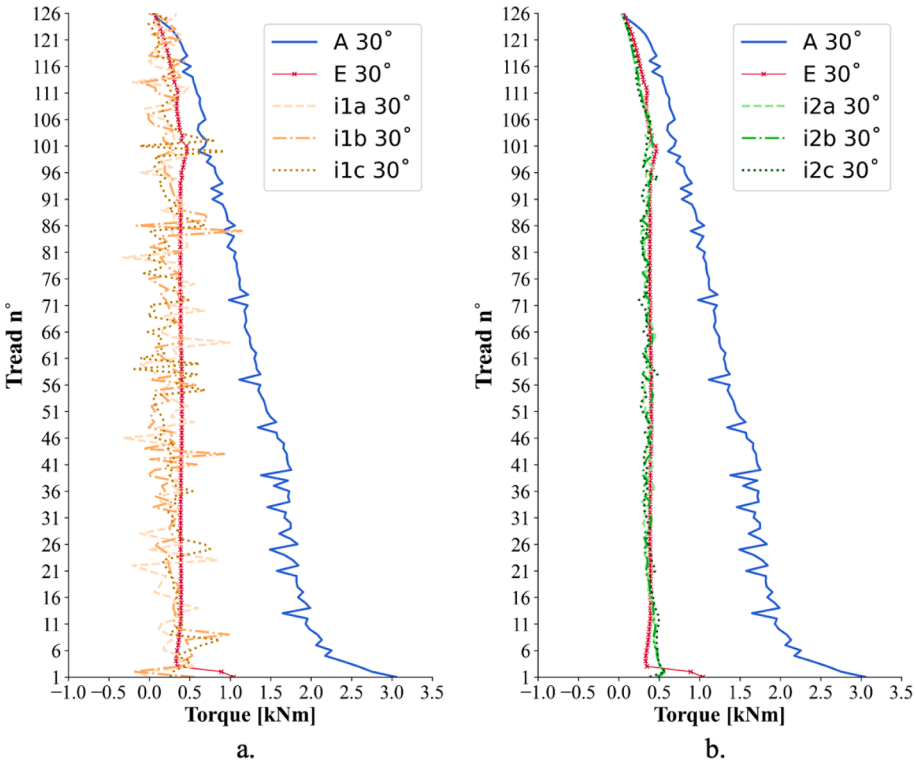

Fig. 20. Torsional moment values in the whole staircase for the wall-tread contact conditions with geometrical imperfections compared with cases "A" and "E": a) "i1a-i1b-i1c" with friction angle equal to 30°; b) "i2a-i2b-i2c" with friction angle equal to 30°.

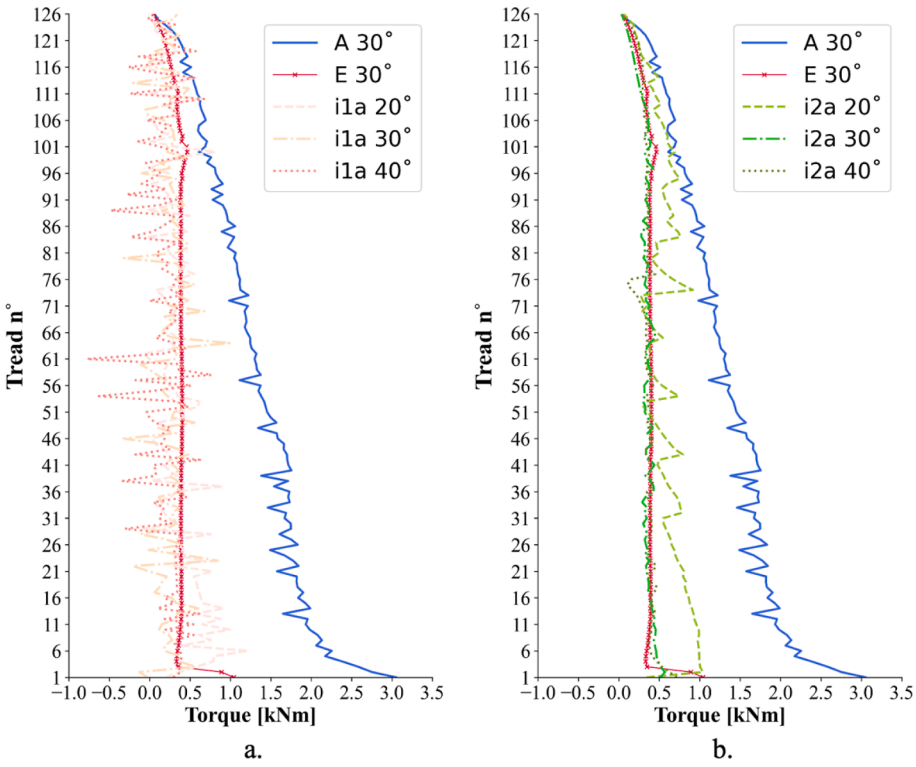

Fig. 21. Torsional moment values in the whole staircase for the wall-tread contact conditions with geometrical imperfections compared with cases "A" and "E": a) "i1a-i1b-i1c" with friction angles equal to 20°-30°-40°; b) "i2a-i2b-i2c" with friction angle angles equal to 20°-30°-40°.

tendency in terms of torsional moment values. As a result, the three models of set2 (i2a, i2b, i2c) in Fig. 20b, generated using higher tolerances (see Table 1), reach torque values almost identical to case "E". Instead, the three models of set1 in Fig. 20a show a different behaviour. Positive spikes in the torsional moment correspond to locations where the magnitude of imperfections is relatively small, and the behaviour is

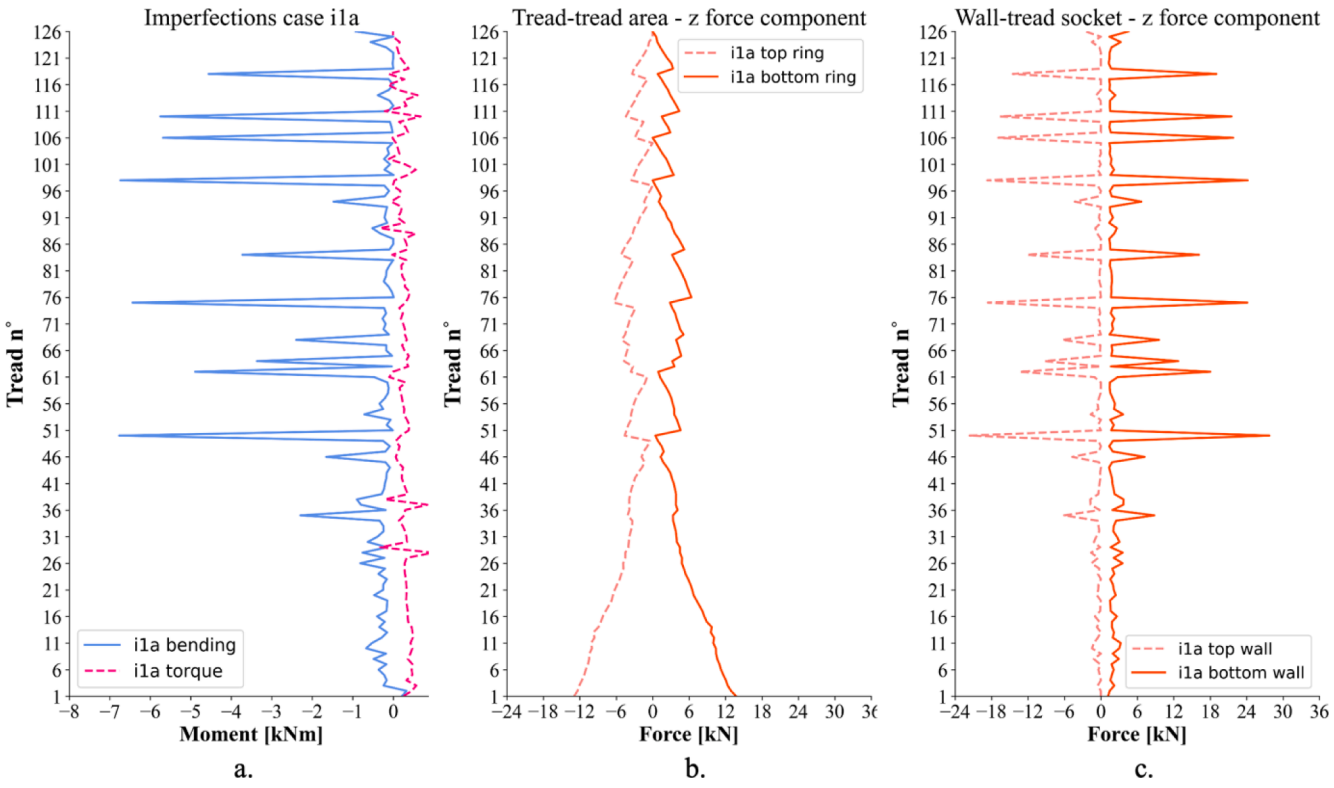

Fig. 22. a) Bending and torsional moment values in the entire staircase for case "i1a" with friction angle equal to 30. b) Magnitude of the ring forces (z component acting at the top and the bottom of each tread). c) Magnitude of the resultant wall forces (z component acting at the top and the bottom of each tread).

similar to the "A" condition. However, in other treads, the torsional moment is smaller than the minimum reached in case "E", and is even negative at some locations. This is caused by imperfect tread-tread contact conditions which modify the location of forces **a** and **b**, inverting the torque's sign and potentially generating local cantilever situations, which increase the bending moment at the wall-tread socket (also see Fig. 22).

Fig. 21 shows the effect of a reduction of the friction angle for the cases with geometrical imperfections. For case "i1a" (Fig. 21a), the friction angle has no considerable effect on the torsional moment, due to the small values of geometrical imperfections. Instead, for case i2a (Fig. 21b) with larger deviations, the torsional moment values increase only in a few locations. In this case, geometrical imperfections have a positive effect, mitigating the effect of a reduced friction angle for some treads.

To better understand what is happening in the case of geometrical imperfections, Fig. 22 shows respectively:

a. The values of the bending and torsional moment;
b. The z component of the contact force acting on the top and bottom of the treads at the tread-tread contact area;
c. The z component of the resultant contact forces acting on the top and bottom of the treads in the wall-tread socket.

Fig. 22 shows the locations of cantilever behaviour due to poor contact conditions. For example, for tread number 61 in Fig. 22a, the torsional moment is almost equal to zero, while tread 62 above has a high value of the bending moment. The same can be observed in Fig. 22b, where the z component of the force at the bottom of tread 62 goes to zero (tread 62 not touching tread 61), and the top component of 61 goes to zero as well (62 not touching the top of 61). In Fig. 22c instead, the spikes of the bending moment are related to an increase of both z components (top and bottom) at the same tread level.

The effects of imperfections observed in this section provide insight for assessment and refurbishment of real spiral staircases, which will be discussed in section 3.8.

3.4. Settlements

A vertical settlement was also applied to the central support, as described in paragraph 2.3.3, to simulate the possible effect if the foundation is poor and could not support the large reaction force at the base of the central ring. Fig. 23 shows that ring support settlement does affect stair behaviour in the lower half of the stair but does not significantly affect the behaviour in the upper half. Notably, the maximum torsional moment is approximately unchanged by the settlement. The effect of larger settlements depends on the magnitude of the wall-tread socket clearance. In Fig. 23a (case "C", top tolerance t1 equal to 0.5 mm), the torsional moment values are affected up to the 45th tread, while in Fig. 23b (case "D", top tolerance t1 equal to 1 mm), the settlement effect reaches the 65th tread. This is as expected, since each tread has more ability to rotate for case "D", due to the increased clearance in the wall socket. The settlement activates the engagement of the treads located at the base of the stair with the wall-tread socket, the y and z components of the contact forces in the socket increase, and there is an increment of the torsional moment. At a certain height in stair (45th tread for case "C" and 65th tread for case "D"), the induced settlement stop propagating, and the torsional moment stays unchanged.

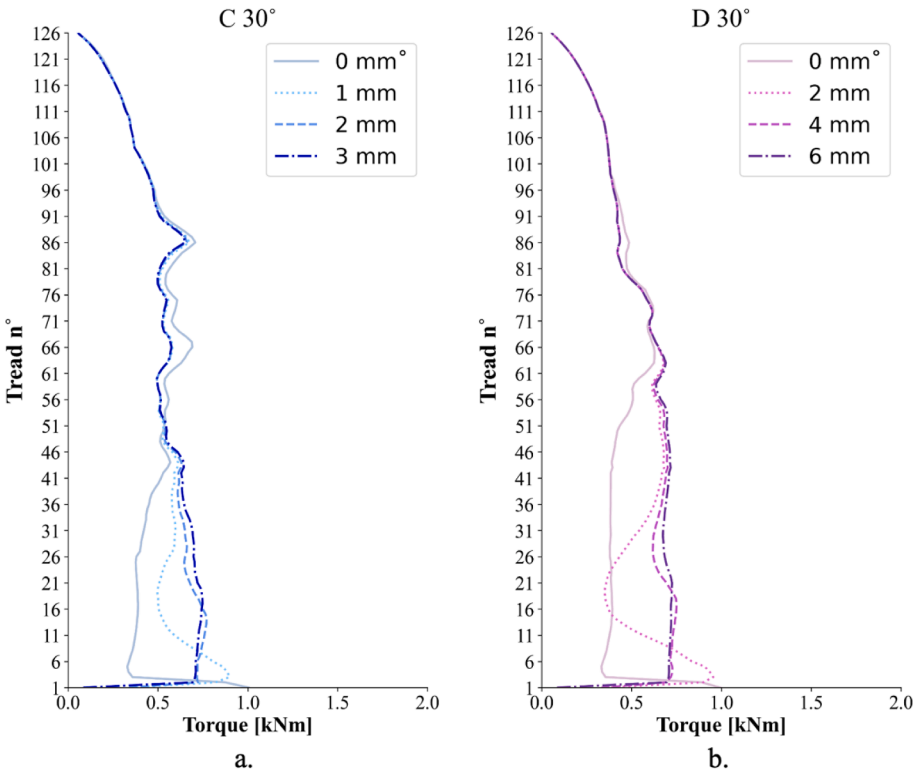

Fig. 23. Torsional moment values in the whole staircase after the vertical settlement of the central support: a) Cases "C" with 0, 1, 2, and 3 mm displacement. b) Cases "D" with 0, 2, 4, and 6 mm displacement.

3.5. Shear and tensile stress and strength

All of the analyses conducted considering the various contact conditions, geometrical imperfections and vertical settlements have shown a maximum value of the torsional moment equal to 3.05 kN-m for case "A" with no clearance and friction angle equal to 30°. However, this value is reached only by a few treads at the bottom of the staircase, while more than 90 % of the treads have a torsional moment lower than 2 kN-m. Even the precarious contact conditions due to imperfections did not generate values higher than case "A", and when cantilever behaviour occurred for models "i1a", "i1b" and "i1c", the torsional moment approached zero. Instead, the bending moment reaches its maximum value.

Shear and tensile strength values are needed to evaluate the capacity of the stair treads to resist these internal forces. [5] assumed shear and tensile strength values of $\tau = 25$ MPa and $\sigma_t = 16$ MPa. Meanwhile, Willoughby [34] used material test data from a few different stone materials to define relationships between the density (an easy to measure property) and other mechanical parameters, such as Poisson's ratio, Young's modulus and flexural strength. These relations can provide a helpful rule approximation to evaluate the strength of the tread material. The density-shear strength relation described by Willoughby [34] is:

$$\tau = 0.018\rho - 32.926 \tag{5}$$

where τ is the shear strength, and ρ is the density of the material. For $\rho = 2700$ kg/m^3, $\tau = 15.7$ MPa, which is below the material shear strength specified by De Serio et al. [5].

In this work, the shear stress has been approximated by considering the cross-section with the smallest area as a right isosceles triangle (see Fig. 24), with the two equal sides of length 0.175 m, as:

$$\tau = (18.05 * M_t)/a^3 = (18.05 * 3.1\ kN - m)/\left(0.0054\ m^3\right) = 10.4\ MPa \tag{6}$$

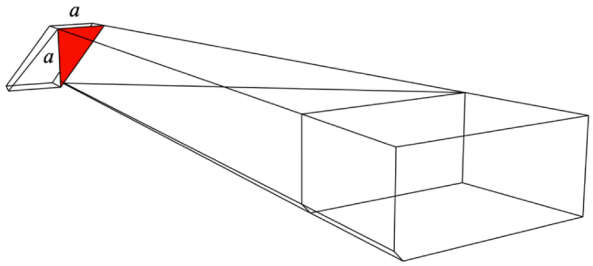

Fig. 24. Triangular cross section used for the calculation of the shear stress due to the torsional moment.

where M_t is the torsional moment and a is the length of the two equal sides of the isosceles triangle (Fig. 24). The value of 10.4 MPa is relatively large but is below the material's shear strength. If we consider the cases with clearance in the wall-tread socket and friction angle equal to 20°, the maximum torsional moment is approximately 1.5 kN-m, which corresponds to shear stress equal to 5 MPa. Finally, the cases with clearance and friction angle equal to 30° have shown a maximum torque value of approximately 1.0 kN-m, corresponding to shear stress equal to 3.3 MPa.

To evaluate how the maximum torsional moment values are related to the material's density, keeping the same geometry, case "A" and "D" have also been analysed with a density equal to 2000 kg/m^3 and 2500 kg/m^3. The values obtained have been used to calculate the shear stress caused by the torsion using (6) and are plotted in Fig. 25 below. In both cases, "A" and "D", there is a linear relationship between the density and the shear stress, but with a different slope. For the same density values, the shear/tensile strength of the material has been calculated using (5). The comparison shows that the torsional moment values reached by the structure in case "D" are below the strength of the material calculated using relation (5) for the three density values, while the values reached

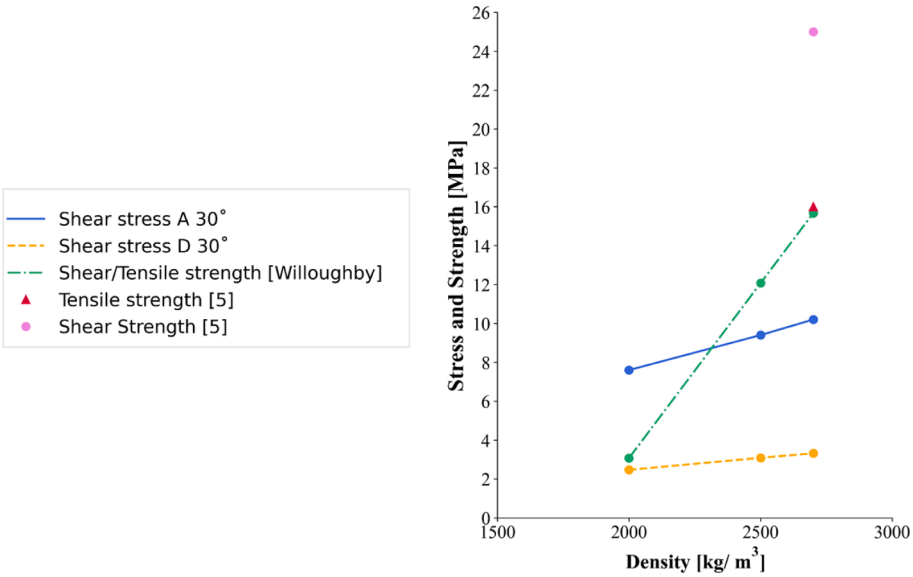

Fig. 25. Comparison between the maximum value of the shear stress calculated for case "A" and "D" with density equal to 2000, 2500 and 2700 kg/m^3, the shear/tensile strength calculated using (5) for same density values, and shear and tensile strength specified by De Serio et al. [5] for the material used in the analyses.

by case "A" are above the shear strength for a density equal to 2000 kg/m^3. Looking at the distance between the shear/tensile strength line and the two stress lines, this comparison gives an idea of the margin of safety of the analysed stair.

Regarding the tensile stress due to bending moment, the maximum value reached is 3 kN-m in the first tread of the case "A", which is influenced by the effect of the boundary conditions, while the maximum value reached by the rest of the staircase is 1.5 kN-m. These values, which correspond to a tensile stress of respectively 0.374 MPa and 0.187 MPa, are quite low compared to the material's tensile strength.

In the case of geometrical imperfections, the imperfect contact conditions in the tread-tread area caused, in cases "i1a", "i1b", and "i1c", a few cantilever situations where the bending moment reaches high values. Obviously, the bending moment value also depends on the height of the tread in the staircase: lower treads have more treads above, causing a higher load and bending moment. The maximum bending moment at the tread-socket interface, caused by imperfections, was 12.2 MPa, which corresponds to a tensile stress of 1.5 MPa. This value is below the tensile strength of the material, but the randomness of imperfections, additional loads on the treads, and the location of the tread in the staircase could generate higher values of the bending moment. For this reason, the tread-tread area is a delicate area that needs attention during assessment and refurbishment, as specified in the next paragraph.

This section has evaluated the magnitude of the internal forces with respect to the strength of the stairs, to gain a perspective on the stability. Of course, the combination of stresses within a tread would need to be evaluated for a detailed evaluation of failure, but the relative magnitude of stresses is sufficient for the discussion here.

3.6. Comparison with overlapping treads

As described in Section 2.2, the structure analysed in this work presents gaps between the treads, which overlap only towards the inner ring. This geometrical feature is not common in URM spiral staircases, which usually have treads overlapping for a few centimetres along their

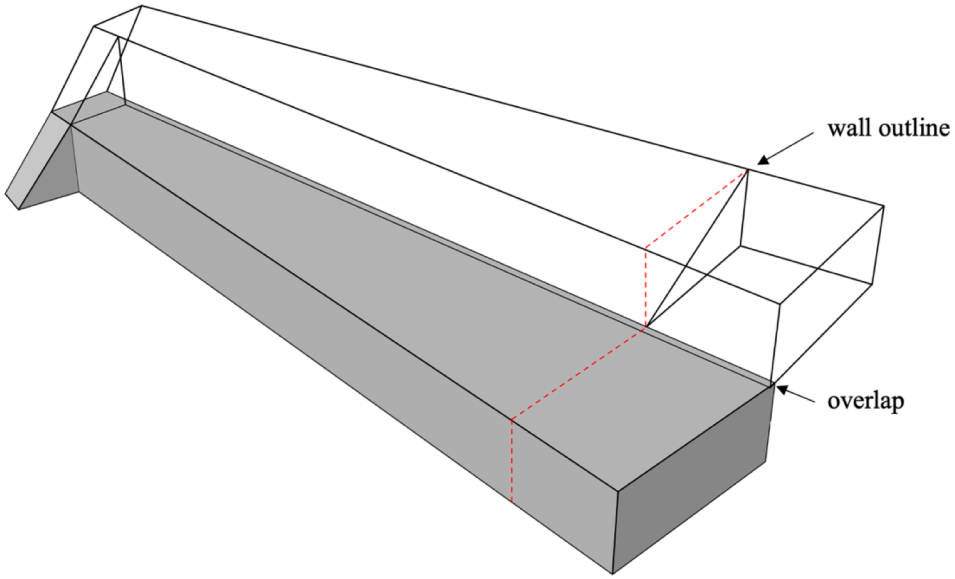

Fig. 26. Digital model of the treads overlapping on the entire length.

full length or gaps filled with mortar. To clarify the influence of a full-length contact on the mechanical behaviour of spiral staircases, the same staircase analysed previously has been modelled with overlapping treads, using a hypothetical overlap of 2 cm, Fig. 26.

The investigation has been conducted on three different cases, using a friction angle equal to 30°:

- A_over - no gaps in the wall-tread socket (same as case A, Fig. 8a);
- E_over - gaps at the top and sides of the wall-tread socket (same as case E, Fig. 8e);
- i1a_over - A_over with geometrical imperfections applied (same ranges as in Set1, Table 1).

Cases A_over and E_over represent the extreme conditions the wall-tread socket could experience in the case of perfect digital geometry. Instead, the case with geometrical imperfections i1a_over, applied to case A_over, simulates more realistic conditions where small deviations compromise the precision of the contacts in the wall-tread socket and between the treads. Furthermore, as already seen in Section 3.3, the case with geometrical imperfections also helps understand the effect of eventual cantilever situations on the mechanical behaviour.

3.7. *Effect of the overlap on the mechanical behaviour*

The analyses conducted on the model with overlapping treads have shown similar results, in terms of torsional moment values, as for the previous case with gaps, except for the case *A_over* with no clearance in the wall-tread socket, Fig. 28a. Fig. 27, which represents, on average, the position of the contact forces transmitted on a tread by the tread above, clarifies the results obtained. As already mentioned in Section 1.1, a variation in the position of the point of application of the contact forces implies a variation of the moment arm lengths with respect to the barycentric axis (torsional moment) and the wall axis (bending moment). Fig. 27a shows that the force experienced by the tread, in the case A, has a bigger distance from the barycentric axis than in cases E and i1a, resulting in higher values of the torsional moment as described in Fig. 16a. In Fig. 27b, instead, which shows the case with overlapping treads, the point of application of the force transmitted by the tread above, for the case *A_over* with no clearance, is situated closer to the middle length of the tread and at a bigger distance from the barycentric axis.

It can be noticed that the position of the contact force in the case *A_over* is outside the overlapping area. This is due to the calculation of the resultant force acting between the treads, which considers the convex hull of all the vertices at the boundaries of the overlapping area. The larger distance of the point of application of the contact force in the case *A_over* results in higher values of the torsional moment, as illustrated in Fig. 28a, which are quite similar to the values obtained by De Serio et al. [5] applying Heyman's approach to the staircase here under investigation, Fig. 2. The torsional moment values calculated indeed are high, and correspond to shear stresses not compatible with the strength of the material. However, the analysis with clearance in the wall-tread socket (case *E_over*) results in lower torsional moment values almost identical to case E. Indeed, Fig. 27b shows that the slight movements allowed by the clearance move the point of application of the force acting on the top of the tread, almost at the same location as for case E (Fig. 27a), with similar values of the torsional moment for the entire staircase Fig. 28a.

In the case of geometrical imperfections (i1a_over), the presence of the overlapping area slightly moves the point of application of the force transmitted by the tread above, closer to the wall axis. Fig. 27b, which compares the bending and torsional moment values calculated in cases i1a and i1a_over, shows the differences mainly in the bending moment values caused by the position of the force. Indeed, at the locations where

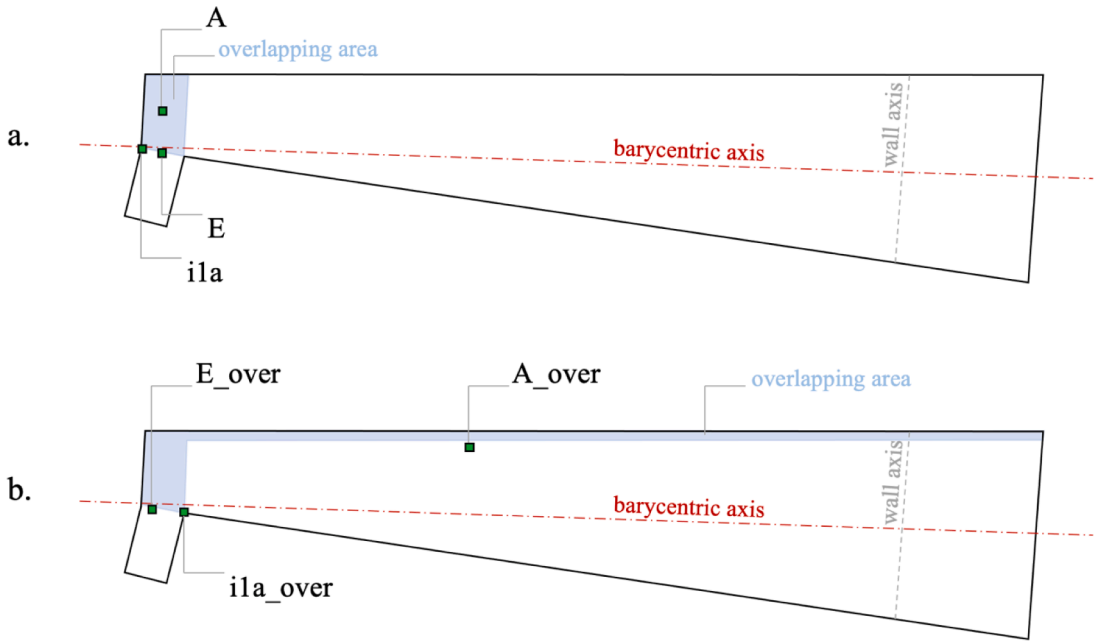

Fig. 27. Positions of the points of application of the forces transmitted by the tread above: a) Cases A, E and i1a (model with gaps between the treads); b) Cases *A_over, E_over, i1a_over* (model with overlapping treads).

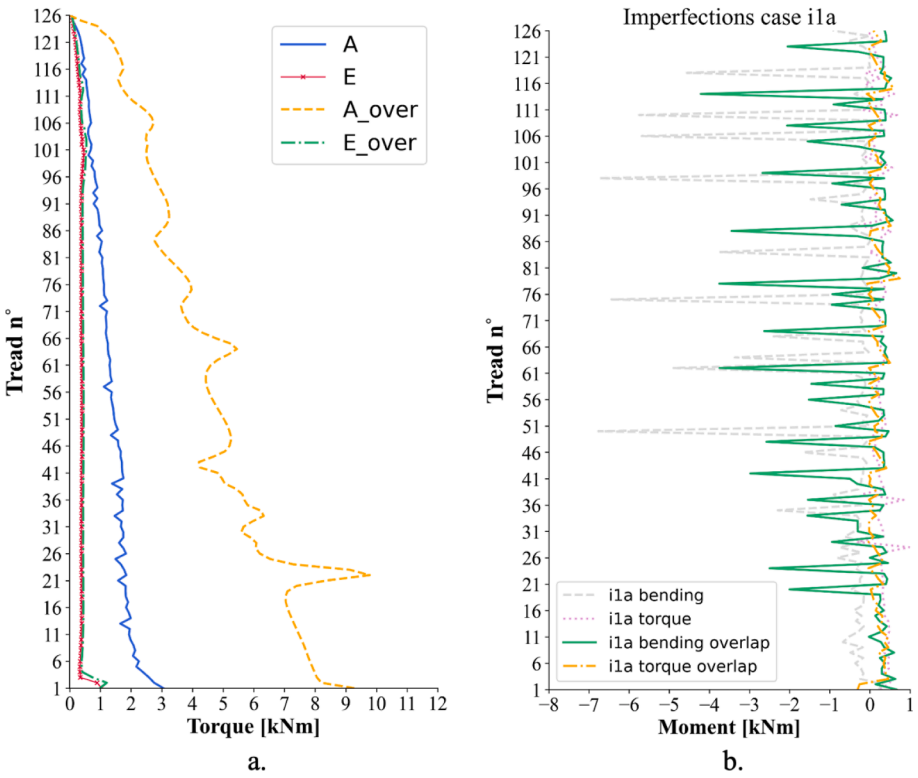

Fig. 28. A) Torsional moment values in the entire staircase for the cases A, E, *A_over, E_over;* b) Bending and torsional moment values in the entire staircase for case i1a and *i1a_over*.

geometric deviations generate cantilevering, the structure experiences lower bending moment values than i1a, where the point of application of the force reaches the maximum distance at the inner ring, Fig. 27a.

3.8. General remarks and assessment strategies

From all the analyses conducted, the main concern for the stability of spiral staircases derives from the shear and tensile stresses that could arise from the torsional moment, and in some specific cases, from the bending moment acting on the treads.

The parametric analysis highlights that the factors that have an influence on the torsional moment are:

1. Imperfect contact conditions between the treads;
2. Imperfect contact conditions between the tread and the wall;
3. Contact friction angle combined with tolerances in the wall-tread sockets.

From a risk perspective, since factor 1 could locally produce high torque values or bending moments due to geometrical deviations, the assessment should first verify the contact conditions between the treads, identifying all the locations where the treads are not entirely in contact. The refurbishment at these locations could prevent live loads or further small displacements from increasing shear or tensile stresses in the treads. A second step in the assessment should check the wall-tread socket conditions (factor 2). However, the analyses indicate that at this location intervention may not be necessary, unless the wall area around the socket presents significant damage. Further, an increase in the service loads of the stair does not necessarily require the refurbishment of the wall-tread socket or the filling of potential gaps in between the tread and the wall. These conclusions can be extended also at the case with treads overlapping along their full length, which in case of no clearance in the wall-tread socket could experience higher values of the torsional moment than the case with gaps between the treads.

Historical masonry structures have stood for centuries, and they have found their equilibrium through small displacements, which occur just after construction due to consolidation and settlement, or continuously throughout their life due to environmental or use changes. The work in De Serio et al. [5] shows how the structure minimises its potential energy through small displacements of the treads. The present work, which shows the reduction of torsional moment caused by introducing tolerances in the wall-tread sockets, demonstrates that the refurbishment of the wall-tread sockets should not over-constrain the treads. Indeed, small displacements in the wall-tread connection help the structure adapt to different boundary conditions without increasing the internal forces.

Finally, if not perfect contact conditions between the treads cause cantilever situations, the refurbishment should always proceed from the bottom to the top of the staircase, since lower "cantilever" treads experience higher torsional moment due to the higher number of treads above.

4. Conclusions

This work investigates the structural behaviour of a 3D digital model of an unreinforced masonry spiral staircase based on the geometry of the stair inside the convent of San Domingo de Bonaval, located in Santiago de Compostela, in Spain. Digital models of the staircase have been analysed using the Discrete Element Modelling software 3DEC by Itasca. The treads and the wall surrounding the staircase have been modelled using 3D solid meshes. This allowed investigation of several wall-tread contact conditions by modelling the clearance between the tread and the socket in the wall, rather than making assumptions on the stiffness of the wall-tread connections. Unlike other studies available in the literature on this topic, the methodology adopted in this work allows for the investigation of a wide range of structural behaviours possible between the fixed and simply supported conditions of the treads. The 3DEC results have been post-processed and visualised using custom Python-

based functions. Afterwards, the contact forces calculated from 3DEC results were used to evaluate the internal forces.

The results show that assuming perfect contact conditions between the treads and the wall leads to a conservative prediction of the torsional moment values in the treads, while gaps and imperfections in the wall sockets allow small displacements of the treads, which reduce the torque and increase the compression force in the inner helical ring of the stair. This suggests that filling possible gaps in the wall-tread socket could potentially have a negative effect on the internal forces. If new load conditions or variations of the boundary conditions happen, the tread will not accommodate any small displacement, and internal forces such as torsional and bending moment could increase.

Cantilever behaviour or an increase of the bending moment can still arise in the case of imperfect contact conditions, especially between the treads. The bending moment arising from potential cantilever situations will reach higher values if the tread cantilevering from the wall is located at the bottom of the stair since more treads rest on it. Consequently, the tread-tread contact area should be the first location to assess. In case of poor contacts, live load conditions could affect the torsional and bending moment, so the contacts should be restored, spreading the contact area.

The investigation of friction showed that structures with friction angles around 20° could experience higher values of the torsional moment. However, it has been seen that slight geometrical deviations, which belong to every real structure, mitigate the influence of a low friction angle, keeping the torsional moment values similar to the case with friction angles equal to 30° or 40°.

The simulation of vertical settlements located in the central area of the tower ("free end" of the treads) caused a local change in behaviour, but did not show a significant increase of the maximum torsional moment experienced by the worst-case tread. The effect of the vertical settlement is clearly related to the tolerances in the wall-tread connection. With a tighter socket, the displacement due to the settlement generates higher values of the torsional moment in a more confined area at the bottom of the stair, since the smaller clearance works to prevent the propagation of the displacement up the stair and fewer treads are affected.

Since the case study considered in this work presents a geometrical feature uncommon among the existing unreinforced masonry spiral staircases, namely the partial gaps between the treads, a model with treads overlapping along the full length has been analysed to identify the differences in the structural behaviour. The investigation has shown that in the presence of tolerances or geometrical deviations, both models experienced similar internal forces. At the same time, the case with tight wall-tread socket conditions reached torsional moment values incompatible with the strength of the material, implying the infeasibility of such a condition.

For the assessment and refurbishment of historic unreinforced spiral staircases, it is worth noting that we should not forget that these structures have existed for centuries and they have likely moved throughout the years by small displacements in response to varying boundary conditions. This paper demonstrates how the structure could respond to these variations in order to inform a refurbishment strategy that is appropriate.

Funding

This work was supported by the SNSF - Swiss National Science Foundation. Project grant n°178953: "Practical Stability Assessment Strategies for Vaulted Unreinforced Masonry Structures".

Declaration of Competing Interest

The authors declare that they have no known competing financial interests or personal relationships that could have appeared to influence the work reported in this paper.

Acknowledgement

The first author would like to thank Prof. Maurizio Angelillo for triggering his interest in the analysis of unreinforced spiral staircases using the discrete element modelling method, and for the interesting discussions about their fascinating structural behaviour.

References

[1] Fitchen J. The construction of Gothic cathedrals: a study of medieval vault erection. University of Chicago Press; 1981.
[2] Palladio A. I quattro libri dell'architettura. Venice: Domenico dè Francheschi.; 1570..
[3] Goethe JW von. Italian Journey, trans. WH Auden and Elizabeth Mayer 1970.
[4] Angelillo M. The equilibrium of helical stairs made of monolithic steps. Int J Archit Herit 2016:10. https://doi.org/10.1080/15583058.2014.988773.
[5] De Serio F, Angelillo M, Gesualdo A, Iannuzzo A, Zuccaro G, Pasquino M. Masonry structures made of monolithic blocks with an application to spiral stairs. Meccanica 2018:53. https://doi.org/10.1007/s11012-017-0808-9.
[6] O'Dwyer D, O'Connor A, Bashorun O. Assessing the probability of material failure in cantilevered stone stairs. Proc. 7th Int. Probabilistic Work. 25-26 Novemb. 2009, Delft, Netherlands, 2009, p. 239.
[7] Price S. Cantilevered staircases. Archit Res Q 1996:1. https://doi.org/10.1017/S1359135500002931.
[8] Price S, Rogers H. James sutherland history lecture-Stone cantilevered staircases. Struct Eng 2005;83:29–36.
[9] Little P, Hough M, Mullarkey E. Stone cantilever stairs-Inspection and analysis of cantilever stairs. Struct Eng 2009;87:26–33.
[10] Price S, Rogers H, Stevenson J. Natural History Museum, Dublin. Structural report into the collapse of a flight of the main staircase. 2007.
[11] Heyman J. The mechanics of masonry stairs. WIT Trans Built Environ 1970:17.
[12] Rigó B, Bagi K. Discrete element analysis of stone cantilever stairs. Meccanica 2018:53. https://doi.org/10.1007/s11012-017-0739-5.
[13] Van Mele T, Liew A, Méndez Echenagucia T, Rippmann M. COMPAS: A framework for computational research in architecture and structures 2017.
[14] Itasca Consulting Group I. 3DEC — Three-Dimensional Distinct Element Code, Ver. 5.2. Minneapolis: Itasca 2016.
[15] Cundall PA. Formulation of a three-dimensional distinct element model-Part I. A scheme to detect and represent contacts in a system composed of many polyhedral blocks. Int J Rock Mech Min Sci 1988. https://doi.org/10.1016/0148-9062(88)92293-0.
[16] Hart R, Cundall PA, Lemos J. Formulation of a three-dimensional distinct element model-Part II. Mechanical calculations for motion and interaction of a system composed of many polyhedral blocks. Int J Rock Mech Min Sci 1988. https://doi.org/10.1016/0148-9062(88)92294-2.
[17] Iannuzzo A, Dell'Endice A, Maia Avelino R, Kao GTC, Van Mele T, Block P. COMPAS Masonry: a computational framework for practical assessment of unreinforced masonry structures. Proc. SAHC Symp. 2020, Barcelona: 2020.
[18] Cabo MCF, Uriel AG, de Miguel M. La triple escalera de caracol en el Convento de Santo Domingo de Bonaval (Santiago, España): Hipótesis de diseño y construcción. Inf La Constr 2017:69. https://doi.org/10.3989/ic.16.119.
[19] Lemos J. DISCRETE ELEMENT MODELING OF MASONRY STRUCTURES 2007; 3058. doi:10.1080/15583050601176868.
[20] Lemos JV. Modelling the dynamics of masonry structures with discrete elements. Open Constr Build Technol J 2016;10:210–9. https://doi.org/10.2174/1874836801610010210.
[21] DeJong MJ, Vibert C. Seismic response of stone masonry spires: computational and experimental modeling. Eng Struct 2012. https://doi.org/10.1016/j.engstruct.2012.03.001.
[22] McInerney J, DeJong MJ. Discrete element modeling of groin vault displacement capacity. Int J Archit Herit 2015. https://doi.org/10.1080/15583058.2014.923953.
[23] Lemos JV. The Basis for Masonry Analysis with UDEC and 3DEC, 2016, p. 61–89. doi:10.4018/978-1-5225-0231-9.ch003.
[24] Block P, Van Mele T, Liew A, DeJong M, Escobedo D, Ochsendorf J. Structural design, fabrication and construction of the Armadillo vault. Struct Eng 2018;96.
[25] Van Mele T, Mehrotra A, Mendez Echenagucia T, Frick U, Ochsendorf JA, DeJong MJ, et al. Form finding and structural analysis of a freeform stone vault. Proc IASS Annu Symp 2016 "Spatial Struct 21st Century" 2016.
[26] Bhooshan S, Bhooshan V, Dell'Endice A, Megens J, Chu J, Singer P, et al. The Striatus arched bridge: computational design and robotic fabrication of an unreinforced, 3D-concrete-printed, masonry bridge. Archit Struct Constr 2022.
[27] Heyman J. The stone skeleton. Int J Solids Struct 1966. https://doi.org/10.1016/0020-7683(66)90018-7.
[28] Simon J, Bagi K. Discrete element analysis of the minimum thickness of oval masonry domes. Int J Archit Herit 2016. https://doi.org/10.1080/15583058.2014.996921.
[29] Sarhosis V, Lemos JV, Bagi K. Discrete element modeling. Numer Model Mason Hist Struct, Elsevier 2019:469–501. https://doi.org/10.1016/b978-0-08-102439-3.00013-0.
[30] DeJong MJ. Seismic Assessment Strategies for Masonry Structures. 2009.
[31] Van Mele T, McInerney J, DeJong MJ, Block P. Physical and computational discrete modelling of masonry vault collapse. Struct Anal Hist Constr 2012;1–3:2552–60.

[32] Dell'Endice A, Iannuzzo A, DeJong MJ, Van Mele T, Block P. Modelling imperfections in unreinforced masonry structures: discrete element simulations and scale model experiments of a pavilion vault. Eng Struct 2021:228.
[33] Dell'Endice A, Iannuzzo A, Van Mele T, Block P. Influence of settlements and geometrical imperfections on the internal stress state of masonry structures. Proc. SAHC Symp. 2020 (postponed to 2021), Barcelona: 2021.
[34] Willoughby A. Collapse of stone staircases. Cambridge University; 2005.